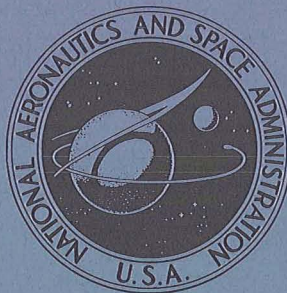


NASA TECHNICAL
MEMORANDUM



NASA TM X-3288

NASA TM X-3288

VISUAL STUDY OF THE EFFECT OF
GRAZING FLOW ON THE OSCILLATORY FLOW
IN A RESONATOR ORIFICE

Kenneth J. Baumeister and Edward J. Rice

Lewis Research Center

Cleveland, Ohio 44135



1. Report No. NASA TM X-3288	2. Government Accession No.	3. Recipient's Catalog No.	
4. Title and Subtitle VISUAL STUDY OF THE EFFECT OF GRAZING FLOW ON THE OSCILLATORY FLOW IN A RESONATOR ORIFICE		5. Report Date September 1975	
		6. Performing Organization Code	
7. Author(s) Kenneth J. Baumeister and Edward J. Rice		8. Performing Organization Report No. E-8339	
9. Performing Organization Name and Address Lewis Research Center National Aeronautics and Space Administration Cleveland, Ohio 44135		10. Work Unit No. 505-03	
		11. Contract or Grant No.	
12. Sponsoring Agency Name and Address National Aeronautics and Space Administration Washington, D.C. 20546		13. Type of Report and Period Covered Technical Memorandum	
		14. Sponsoring Agency Code	
15. Supplementary Notes			
16. Abstract A visual study of the effect of grazing flow on the oscillatory flow in an orifice was performed in a plexiglass flow channel with a single side branch Helmholtz resonator using water as the fluid medium. An oscillatory flow was applied to the resonator cavity, and color dyes were injected in both the orifice and the grazing flow field to record the motion of the fluid. The flow regimes associated with linear and nonlinear (high sound pressure level) impedances with and without grazing flows were recorded by a high-speed motion-picture camera. Appreciable differences in the oscillatory flow field were seen in the various flow regimes. With high grazing flows, the outflow and inflow from the resonator cavity were found to be asymmetric. The visual study confirms the measured data reported in the literature that the jet energy loss during flow into the resonator cavity is much larger than the loss for ejection from the cavity into the grazing flow. For inflow into the resonator cavity, the effective orifice area was significantly reduced.			
17. Key Words (Suggested by Author(s)) Helmholtz resonator Grazing flow resistance Water simulation		18. Distribution Statement Unclassified - unlimited STAR Category 71 (rev.)	
19. Security Classif. (of this report) Unclassified	20. Security Classif. (of this page) Unclassified	21. No. of Pages 28	22. Price* \$3.75

* For sale by the National Technical Information Service, Springfield, Virginia 22161

VISUAL STUDY OF THE EFFECT OF GRAZING FLOW ON THE OSCILLATORY FLOW IN A RESONATOR ORIFICE

by Kenneth J. Baumeister and Edward J. Rice

Lewis Research Center

SUMMARY

A visual study of the effect of grazing flow on the oscillatory flow in an orifice was performed in a plexiglass flow channel with a single side branch Helmholtz resonator using water as the fluid medium. An oscillatory flow was applied to the resonator cavity, and color dyes were injected in both the orifice and the grazing flow field to record the motion of the fluid. The flow regimes associated with linear and nonlinear (high sound pressure level) impedances with and without grazing flows were recorded by a high-speed motion-picture camera. Appreciable differences in the oscillatory flow field were seen in the various flow regimes. With high grazing flows, the outflow and inflow from the resonator cavity were found to be asymmetric. The visual study confirms the measured data reported in the literature that the jet energy loss during flow into the resonator cavity is much larger than the loss for ejection from the cavity into the grazing flow. For inflow into the resonator cavity, the effective orifice area was significantly reduced.

INTRODUCTION

In recent years, for both rocket engine stability and reduction of jet aircraft engine noise, the operation of Helmholtz resonators has been the subject of much research. Numerous investigators have conducted experiments in which various correlations of the resistance and reactance have been developed. References 1 to 8 comprise an excellent review of the state of the current understanding of Helmholtz resonators as duct boundary conditions.

Despite considerable progress during the last decade, there is still much unknown concerning the mechanism of acoustic energy removal by the resonator in the presence of the usual grazing flow. Various flow conditions can occur in and

near the resonator orifice depending on the geometry of the resonator, the sound pressure level of the acoustic oscillation, the magnitude of the grazing flow, and the frequency of excitation. These factors make it difficult to formulate a model (or models) of the impedance of the Helmholtz resonator.

Much more detailed information is needed regarding physical flow interaction process occurring near the mouth of a Helmholtz resonator in the presence of grazing flow. Visual studies were expected to be helpful in developing realistic models of fluid flow motion necessary for any analytical treatment. A brief flow visualization study has therefore been performed and reported herein using water as the fluid medium in a transparent test section of a Helmholtz resonator and flow channel. This dynamic flow visualization extends the steady-flow visualization study reported in reference 6. In the present investigation, an oscillatory flow was applied to the back cavity of the Helmholtz resonator, and three different color dyes were individually or simultaneously injected at points in the free stream and orifice. The motion of the dyes and thus the fluid are recorded by a high-speed camera. Individual motion-picture frames are presented in this report to illustrate the flow regimes.

The motion picture from which the still photographs in this report were taken may be obtained by contacting the authors.

SYMBOLS

- C speed of sound, m/sec
- C_{De} discharge coefficient in presence of grazing flow
- C_{Do} discharge coefficient without grazing flow
- D_H hydraulic diameter of duct, m
- d orifice diameter, m
- f frequency, Hz
- l length of orifice, m
- p static pressure, N/m^2
- p_c chamber pressure, N/m^2
- p_∞ free stream static pressure, N/m^2
- R orifice resistance, $kg/m^2/sec$

t	time, sec
v	velocity, m/sec
\bar{v}_{jet}	average jet velocity in orifice (volume flow rate/area of orifice), m/sec
v_{∞}	grazing flow velocity or average water channel velocity, m/sec
ρ	density, kg/m ³
χ	reactance
ω	circular frequency, rad/sec

APPARATUS AND PROCEDURE

Figure 1 is a schematic diagram of the test apparatus. The apparatus is essentially a once-through water flow system. Details of the main water flow test channel are shown in figure 2, while the details of the resonator cavity are shown in figure 3. As seen in figure 3, the orifice hole is a square 1.27 by 1.27 cm. The square geometry rather than a circular one was chosen for ease in photographing the flow.

Three different color dyes can be injected into the flow field (see fig. 1). The dye flows under the action of gravity to the dye injection locations marked in figure 3. The needle valve shown in figure 1 was adjusted to prevent jetting of the dye so as to minimize any disturbance to the flow field. Water soluble dyes were used.

The flow oscillations to the resonator cavity, intended to simulate acoustic oscillations, are driven by a servocontrolled hydraulically operated piston, as shown in figure 1. The piston could be oscillated from 0.1 to 50 hertz. For the purpose of these experiments, the frequency was set at 2 hertz. At higher frequencies (greater than 10 Hz), the equipment had a tendency to vibrate. At frequencies lower than 2 hertz, the resulting pulse was not sinusoidal. This latter effect was thought to occur because of resonance in the fluid lines.

For convenience, in most tests the oscillatory flow was applied to the resonator cavity rather than the main flow stream. In this manner, the magnitude of the flow oscillation in the orifice could be precisely controlled by varying the stroke of the piston. Using this procedure resulted in the resonator cavity being left completely full of water with no need for an air bubble to provide compliance. In addition, some tests were run with the flow oscillation introduced into the main fluid stream. With main channel excitation, some air must be maintained in the back cavity to provide

compliance so that a main stream flow perturbation will produce flow into the back cavity. As will be shown by photographs in a later section of this report, the same type of flow profiles in the orifice occurred whether the flow oscillation was introduced in the back cavity or in the main stream.

The grazing flow was measured with a turbine flowmeter and the frequency and displacement of the piston were also measured. The high-speed motion-picture camera was positioned adjacent to the resonator cavity. The velocity field in the orifice and in the main water channel were determined from the high-speed motion pictures by following the movement of the dye.

In the entrance region of the main flow channel, a system of screens and baffles was added, as shown in figure 4, to produce an initially uniform velocity profile in the vicinity of the resonator. The velocity profile adjacent to the orifice was determined in an approximate manner by injecting dye at various transverse positions in the flow channel and recording the movement of the leading edge of the dye as a function of time on the motion-picture film. The smoothed velocity profile is shown in figure 5. As seen in figure 5, the "boundary layer" extends approximately 0.3 cm from the wall. This gives a ratio of boundary thickness to orifice size of around 0.25, which is small compared to the corresponding ratio in actual flow ducts. Although this may change the magnitude of the resistance, it should not change the general characteristics of the flow regimes.

In the transverse direction (2.54-cm dimension) the boundary was estimated to be of approximately the same size. Consequently, the side boundary layer does not infringe upon the open area of the orifice.

During a run, the grazing flow velocity in the main channel was first set. Next, the frequency (2 Hz) and amplitude of the resonator flow perturbation were set. Finally, the valves to the dye reservoirs were opened. When desired, a high-speed motion-picture camera recorded the flow pattern. Generally, the camera was run at 500 frames per second.

SCALING CONSIDERATIONS

The intent of this study was to provide a visualization and hence a better understanding of the air flow process in a resonator orifice in the presence of a grazing steady flow. It is important to consider whether the water system simulates an air system.

For both air and water, the dimensionless resistance and reactance are correlated in figure 6 which is reproduced from reference 9. Two sets of data are shown with air the open symbols and water the solid symbols. The circles stand for resistance, while the squares represent reactance. It is obvious that, if the quantities are properly scaled, the resistance and reactance behavior for systems with both fluids are identical. That is, dividing both the resistance and reactance by the quantity $\rho\omega d$ brings both the air and water data into correlation. This factor was found in reference 9 by theoretical consideration of the momentum and continuity equation.

The reactance data shown in figure 6 apply to the case of a sharp-edged orifice, for which the length of the orifice can be assumed to be near zero. However, theoretical considerations in reference 9 suggest that the characteristic length of $(l + d)$ be used to nondimensionalize, that is, $\chi/\rho\omega(d + l)$ and $R/\rho\omega(d + l)$ should be the proper dimensionless groups to correlate the data for a wider range of orifice length to diameter ratios. From this theoretical consideration and the experimental results displayed in figure 6, proper scaling of both reactance and resistance can be considered. Scaling of the reactance will be considered first.

As seen in figure 6 the dimensionless orifice reactance is relatively constant at a value near unity for all values of $(v_{jet}/\omega d)$. Therefore,

$$- \frac{\chi}{\rho\omega(d + l)} \approx 1$$

or

$$- \frac{\chi}{\rho\omega d} \approx (1 + \frac{l}{d})$$

Therefore, for a given orifice size, for similarity of reactance between water and air systems, the ratio of orifice length to diameter should be equal. In the water simulation study to follow, the length to diameter of the orifice is 0.5; thus, the flow field will simulate an air orifice with the same ratio. The l/d ratio of 0.5 is within the practical range for typical noise suppressors.

The resistance data shown in figure 6 are a function of the parameter $v_{jet}/\omega d$. Again, with sufficient accuracy for the purposes here, from figure 6 and theoretical considerations of l/d , it follows that

$$\frac{R}{\rho\omega d(1 + \frac{l}{d})} \approx \left(\frac{v_{\text{jet}}}{\omega d}\right)$$

to ensure scaling between air and water system .

As an example, consider an oscillating water system with an orifice jet velocity of 0.3 meter per second (typical of those induced in the water simulation rig), a frequency f equal to 2 hertz (the value used in the flow visualization study) or $\omega = 4\pi$ radians per second and an orifice diameter of 1.27 cm (the effective hydraulic diameter of the orifice hole used in the visualization study, see fig. 3). Using the following values:

$$\frac{v_{\text{jet}}}{\omega d} \approx \frac{6}{\pi}$$

the corresponding scaled air system with $f = 2000$ hertz ($\omega = 4000\pi$ rad/sec) and $d = 1.27$ millimeters would require $\bar{v}_{\text{jet}} = 30.5$ meters per second which would require about 150-decibel sound pressure level. These are certainly typical numbers which might be encountered in an acoustic liner.

The preceding discussion, although providing convincing evidence that air-water system similitude can be attained, does not consider the effect of grazing flow past the orifice. Similarity with grazing flow may be inferred from the following arguments: The Reynolds number for the water system $v_{\infty}d/\nu$ in figure 5 is about 4000. The Reynolds number for an air system with an orifice diameter of 1.27 millimeters and a grazing flow velocity of 50 meters per second has the same Reynolds number. Thus, the ratio of dynamic to viscous forces is similar. Figure 7 is reproduced from reference 6. This shows that the orifice discharge coefficient C_{De} can be correlated with the ratio of orifice velocity to grazing flow velocity over a wide range of grazing flow velocities (12.9 to 68.4 m/sec shown here). Separate curves are required, however, for the inflow and outflow portion of the cycle. For high through flows, these curves approach the turbulent discharge coefficient (ref. 10, p. 261) for no grazing flow labeled C_{Do} (dashed line in fig. 7). Figure 7 was obtained with an airflow system.

Figure 7 implies that the ratio of orifice flow to grazing flow fixes the orifice discharge coefficient, thus the orifice blockage and therefore the orifice resistance

(see ref. 6). This implies that, if the water flow system reproduces the orifice to grazing flow velocity ratio of an air system, the flows are likely to have similitude. The two stream (orifice-grazing) momentum ratio will be reproduced thus implying dynamic force similarity.

ORIFICE FLOW VISUALIZATION

The following several figures summarize the oscillatory flow regime for a simulated resonator orifice. The figures contain single frames taken from a motion-picture study.

Photographs of oscillating orifice flow without the presence of grazing flow will be presented showing both the linear and nonlinear flow regimes. The linear regime is defined as that flow regime where the energy dissipation is due to viscous scrubbing losses on the surfaces in the vicinity of the orifice. On the other hand, the nonlinear regime is defined as that flow regime where the energy losses are primarily by loss of the kinetic energy heat due to the dissipation of the eddies formed by the sudden expansion.

The linear flow regime is usually not of much practical interest with perforated acoustic liners, but is presented for completeness and to form a contrast with the higher-amplitude (nonlinear) flows to be shown later.

Next, photographs of oscillating orifice flow with grazing flow will be presented. Orifice flow regimes with a grazing flow on one side of the orifice are of much more practical interest for acoustic suppressor applications in turbomachinery than the flow regimes without grazing flow. In fact, the acoustic resistance developed by the nonlinear interaction between the orifice flow and the grazing flow makes perforated plate liners usable as wide-band suppressors. Without the grazing flow these same perforates provide low resistance suppressors (ref. 2) which are narrow banded suppressors of more limited use.

The photographs of the oscillating orifice flow in the presence of grazing flow will be presented showing both intermediate and high amplitude flow regimes. By definition, the intermediate amplitude flow regimes occur when the ratio of the maximum orifice velocity to the grazing flow velocity is less than 0.5. In this situation, C_{De} is approximately limited to the rising portion of the curve as shown in figure 7. The high amplitude flow regime occurs when this ratio is greater than 0.5, where C_{De} is approximately constant.

No Grazing Flow

Linear flow regime. - The flow regime in which the orifice oscillatory particle displacement is extremely small and in which no grazing flow is present is shown in figure 8. Note that the dye injection into the orifice remains mainly in the orifice due to the small oscillatory displacement. Because there is an absence of flow separation, the pressure drop across the orifice is dissipated mainly in viscous scrubbing losses. Some of the dye-carrying fluid is seen to have attached to the outer channel surface above the top of the orifice, and additional area over that of the orifice itself is involved in the scrubbing losses. Although this regime is not practically important, as mentioned earlier, this regime represents the theoretically lower limit for the losses in an oscillating orifice flow.

Nonlinear flow regime. - A more practical flow regime is illustrated in figure 9. In figure 9, the "nonlinear" oscillatory flow is shown which results from large-amplitude displacements. On both the inflow and outflow the fluid is accelerated and thus a drop in static pressure occurs in the orifice. Due to the sudden area expansion at the orifice exit, the accelerated flow separates upon discharge in either direction. For practical purposes, in the resonator cavity the static pressure of the jet and the ambient fluid are nearly equal, and no pressure recovery occurs. The jet kinetic energy is dissipated (ref. 10).

The motion-picture study, from which the still-photograph sequences were taken, clearly shows the large eddies (high turbulence) dissipating the kinetic head of the jet in the resonator cavity, similar to the earlier work of reference 8.

The motion-picture sequences also reveal that a counterflow exists in the resonator cavity near the orifice at the start of the cycle for resonator outflow. This is illustrated by arrows in figure 9 for the frames $0.192 \leq t \leq 0.312$. Along the centerline of the orifice, inertia keeps the inflow moving towards the back cavity wall, while at the same time fluid flows outward from the back cavity into the orifice near its edges.

At the maximum flow ($t = 0.574$ sec in fig. 9), a vena-contracta occurs in the orifice. At this condition, the peak velocity is greater than that which would be calculated from the flow rate with the orifice running full.

Grazing Flow Regimes

Intermediate amplitude regime. - This regime is illustrated in figure 10 which shows one cycle with both inflow and outflow. Recall, by definition the intermediate regime occurs where the ratio of jet velocity to grazing flow velocity is less than 0.5. The resistance due to grazing flow may be viewed qualitatively as an orifice blockage effect which is evident in the sequence in figure 10.

During the inflow portion of the cycle ($t = 0$ to 0.236 sec), the axial momentum (vertical) of the grazing flow makes it difficult for the fluid to negotiate the turn into the orifice. This results in a large separation or dead flow region at the lower side of the orifice which effectively reduces the area of inflow. The inflow region is seen to be limited to the small channel of the top of the orifice.

On the outflow portion of the cycle ($t = 0.236$ to 0.5 sec), the orifice flow is seen to encounter the large axial momentum of the grazing flow which must be displaced before the orifice flow can emerge. Rogers and Hersh (ref. 6) model this portion of the cycle as a lid extending over the orifice with a hinge on the bottom corner. The orifice flow is limited to the small channel emerging from the top of the orifice again illustrating the blockage effect of the grazing flow.

The advantage of oscillating flow visualization over that of steady flow can be seen by the sequence $t = 0.178$ to 0.312 second in figure 10. At $t = 0.178$ second, high velocity inflow exists at the top of the orifice while a dead region occurs at the bottom. As time progresses, the pressure drop across the orifice changes to a higher pressure on the left of the orifice than on the right (favors outflow). The high velocity jet regions cannot be immediately stopped and reversed. The dead region can, however, be more quickly accelerated to form an outflow. Thus there is an instant in the cycle where inflow exists on the top of the orifice and outflow exists on the bottom such that the net flow through the orifice is zero. Around this zero flow condition, a resistance against time (or net flow) history should be produced which is continuous. In effect, the two-dimensional quality of the dynamic flows will remove the discontinuity of resistance at zero through flow which was observed by Budoff and Zorumski (ref. 4) and Rogers and Hersh (ref. 6).

High amplitude regime. - With a higher oscillating flow amplitude than the previous example the minimum effective flow area of the orifice is seen to be increased (fig. 11). The flow is seen to be qualitatively the same as in figure 10, except that both the inflow and outflow channels are expanded to a larger portion of the orifice

area. That is, the dye streamline shown in figure 11 ($t = 0.226$ sec) is bent at a steeper angle on entering the orifice for the higher amplitude flow oscillation. If the oscillatory amplitude were increased sufficiently, the axial momentum (vertical) of the grazing flow would become insignificant in comparison to the available transverse (horizontal) pressure gradient and the flow regime of figure 9 (no grazing flow) would be reproduced. Thus, in the limit of high orifice flow amplitude the flow region for zero-grazing flow is reproduced.

Grazing Flow Captured by the Orifice

In figure 12 another dye jet was placed in the flow with an intermediate flow oscillation applied to the resonator cavity. The dye injection point was spaced sufficiently far from the wall so that the orifice just captured the streamline represented by the dye jet at the peak of the orifice inflow. At $t = 0.218$ second the remote dye jet is seen to be split between orifice inflow and flow downstream past the orifice. The spacing of the streamlines in the grazing flow and in the orifice is seen to change little (see also $t = 0.268$ sec), suggesting that the velocities are also similar. Thus the full grazing flow velocity seems to be attained in the orifice during the inflow part of the cycle. Of course, in general this will be a function of the ratio of boundary layer thickness to orifice size.

During the outflow, the outward deflection of the grazing flow streamline is apparent ($t = 0.364$ to 0.50 sec). Because of the limited size of the experimental flow channel, the total grazing flow rate will fluctuate slightly; however, this did not affect the basic results of the visual study.

The amplitude of the flow oscillation was increased into the high amplitude range ($v_{jet}/v_{\infty} > 0.5$) and the dye jet position was increased to 0.9 centimeter to map out the dividing streamline, as seen in figure 13(a). Again the streamline spacing seems to be preserved during the inflow. In figure 13(b) the remote dye jet was moved towards the wall while the high pressure amplitude was maintained. The flow between the dye jet and wall again seems to be of constant velocity as it is diverted into the orifice. As before, this behavior will in general be a function of the ratio of boundary layer thickness to orifice size.

Grazing Flow Oscillation

The previous examples (figs. 8 to 13) were obtained with the oscillatory flow introduced into the back cavity. This was done to maintain better control over the orifice flow without having to contend with back cavity resonance. The question will often arise: does this back cavity driving provide an analog to the orifice flow since this case has zero compliance and presents the inverse of the true suppressor configuration where oscillatory driving occurs from the main channel?

The driving (oscillation) flow was applied to the main channel and some results are shown in figure 14. Since the water is incompressible and the back cavity was closed, an airspace was provided within the cavity to give compliance and enable orifice flow. In figure 14(a) the system is driven at 1 hertz. Very little orifice response was obtained at this frequency. In figure 14(b) the frequency was increased to 5 hertz and large orifice flows were observed. In this case, the resonator is thus much like that of a gaseous resonator system in that it responds differently to different frequencies with the largest response occurring when the excitation frequency corresponds to the resonance frequency of the resonator cavity. However, note that when the resonator does respond, such as in figure 14(b), the orifice flow looks very similar to that of the cavity-driven system such as shown in figure 11. It was thus concluded that when orifice flow alone is the subject of interest, driving the back cavity does provide a valid orifice analog.

Qualitative Resistance Variation

The orifice flow regimes that were previously discussed are qualitatively summarized by superimposition upon the resistance characteristics of an orifice in figure 15. Without grazing flow ($v_{\infty} = 0$) the orifice flow patterns are symmetrical across the orifice. Inflow and outflow are identical except, of course, for direction. The resistance is defined by the usual definition of pressure difference ΔP divided by the average jet velocity (ref. 7).

With grazing flow $v_{\infty} > 0$, the inflow and outflow are quite different. For inflow, flow blockage reduces the effective area; thus, for the same average jet flow, the kinetic head is larger and thus the energy loss in the resonator cavity is greater since there is very little pressure recovery in the back cavity. Thus, the resistance is high. For outflow the jet is turned and the emerging streamline is restricted in area by the grazing flow. The resistance is considerably reduced over that of the

inflow portion of the cycle. This should be expected since only a part of the kinetic energy of the jet is lost.

Herein, the values of the resistance curves (for $v_{\infty} > 0$) are assumed continuous through $\bar{v}_{jet} = 0$. Experiments (ref. 6) using steady flow show a discontinuity across $\bar{v}_{jet} = 0$ when going from inflow to outflow. However, the evidence for assuming a continuous resistance curve is the counterflow found in the orifice under dynamic flow conditions. Although $\bar{v}_{jet} = 0$, there was shown to exist a large inflow in one side of the orifice while a large outflow exists on the other side (see fig. 10; $t = 0.236$ sec).

SUMMARY OF RESULTS

By means of colored dye traces, photographic sequences illustrate the detailed structure of an oscillating orifice flow with and without the presence of a grazing flow field. Specifically, the following major results were found:

1. For flow into the resonator with grazing flow, the orifice flow area blockage is a strong function of both the amplitude of the pressure oscillation and the magnitude of the grazing flow.

2. Different flow regimes occur for flow oscillation with and without grazing flows. Also, with grazing flow, flow into the resonator is different from the flow out of the resonator. Thus, in modeling these flows, different flow models must be used for each flow regime.

3. As shown in the photographic sequences, at the crossover from inward to outward flow ($v_{jet} = 0$), flow exists simultaneously inward and outward in different parts of the orifice. Thus, no discontinuity in resistance will exist in an oscillating system when the average jet velocity approaches zero from either the inflow or outflow directions.

Lewis Research Center,

National Aeronautics and Space Administration,

Cleveland, Ohio, May 21, 1975,

505-03.

REFERENCES

1. Groeneweg, J. F.: Current Understanding of Helmholtz Resonator Arrays as Duct Boundary Conditions. Basic Aerodynamic Noise Research, Ira R. Schwartz, ed., NASA SP-207, 1969, pp. 357-368.
2. Rice, E. J.: A Model for the Acoustic Impedance of a Perforated Plate Liner with Multiple Frequency Excitation. Presented at Acoustical Soc. Am., Fall Meeting, Denver, Color., Oct. 19-22, 1971 (also NASA TM X-67950).
3. Feder, Ernest; and Dean, Lee W., III.: Analytical and Experimental Studies for Predicting Noise Attenuation in Acoustically Treated Ducts for Turbofan engines. NASA CR-1373, 1969.
4. Budoff, Marvin; and Zorumski, William E.: Flow Resistance of Perforated Plates in Tangential Flow. NASA TM X-2361, 1971.
5. Armstrong, D. L.: Acoustic Grazing Flow Impedance Using Wave Guide Principles. (D3-8684, Boeing Co.; NAS3-14321.), NASA CR-120848, 1971.
6. Rogers, Thomas; and Hersh, Alan S.: The Effect of Grazing Flow on the Steady State Resistance of Square-Edged Orifices. AIAA Paper 75-493, Mar. 1975.
7. Ingard, Uno; and Ising, Harmut: Acoustic Nonlinearity of an Orifice. J. Acoust. Soc. America, vol. 42, no. 1, 1967, pp. 6-17.
8. Ingard, Uno; and Labate, S.: Acoustic Circulation Effects and Nonlinear Impedance of Orifices. J. Acoust. Soc. America, vol. 22, no. 2, Mar. 1956, pp. 211-218.
9. Hersh, Alan S.; and Rogers, Thomas: Fluid Mechanical Model of the Acoustic Impedance of Small Orifices. AIAA Paper 75-495, Mar. 1975.
10. Rouse, Hunter: Fluid Mechanics for Hydraulic Engineers. Dover, 1961.
11. Thurston, G. B.; Hargrove, Jr., L. E.; and Cook, W. D.: Nonlinear Properties of Circular Orifices. J. Acoust. Soc. America, vol. 29, no. 9, 1957, pp. 992-1001.

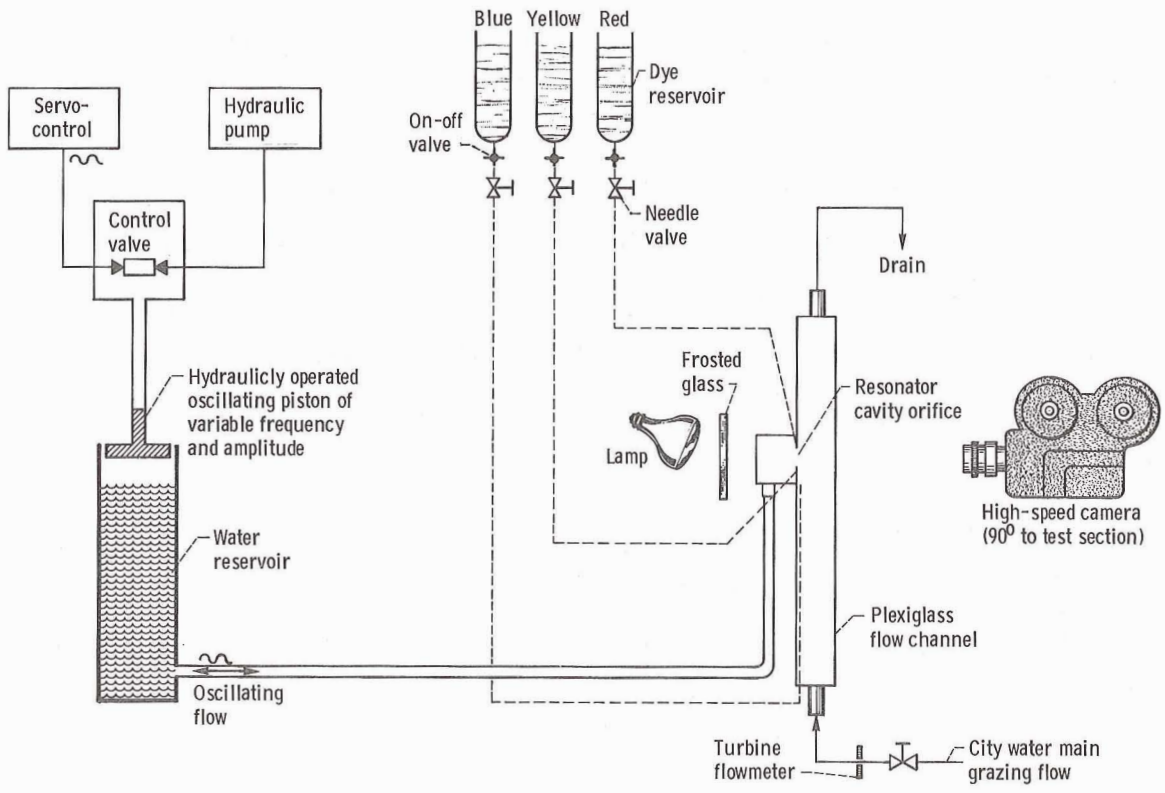


Figure 1. - Apparatus schematic for visualizing oscillatory flow in resonator orifice in presence of grazing flow.

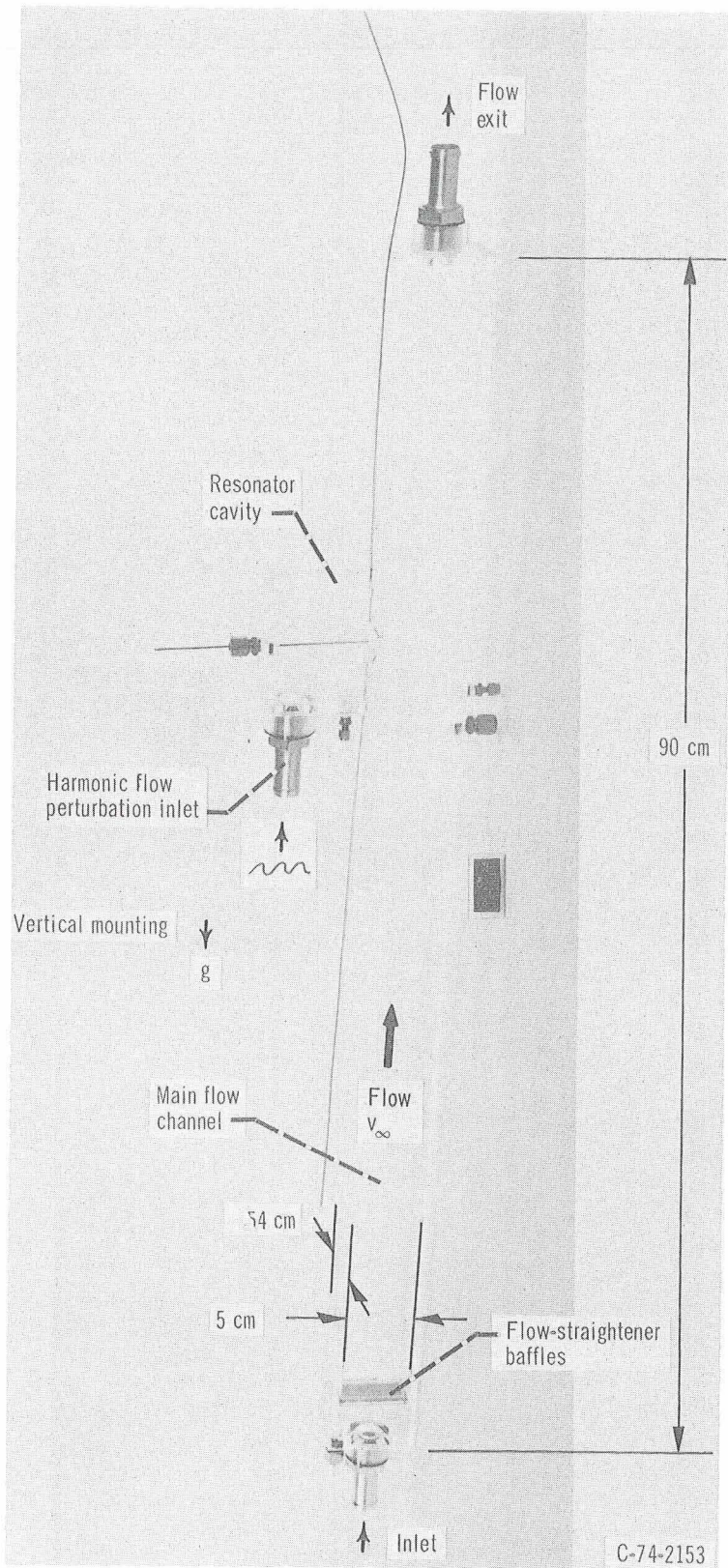


Figure 2. - Flow channel.

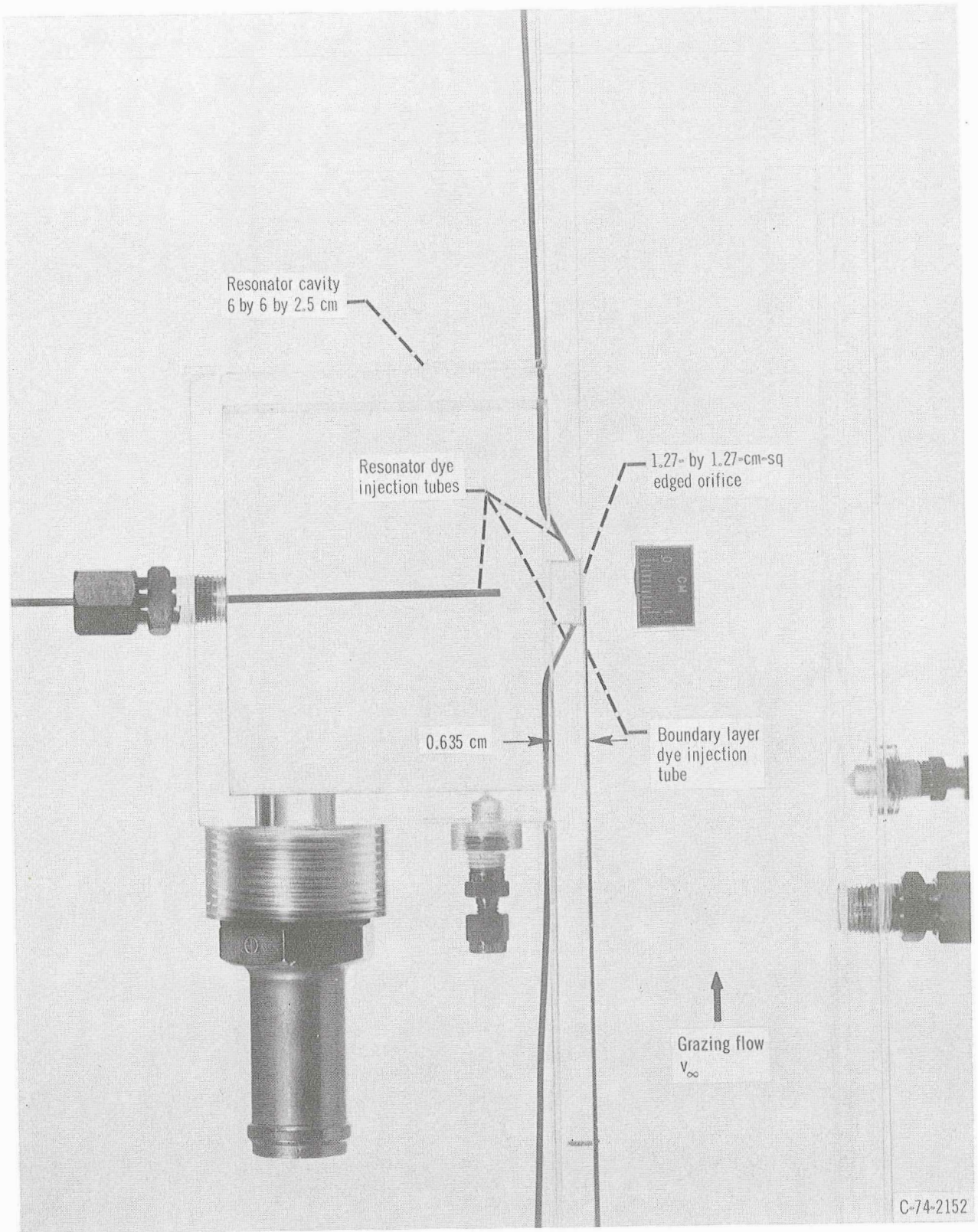


Figure 3. - Resonator cavity.

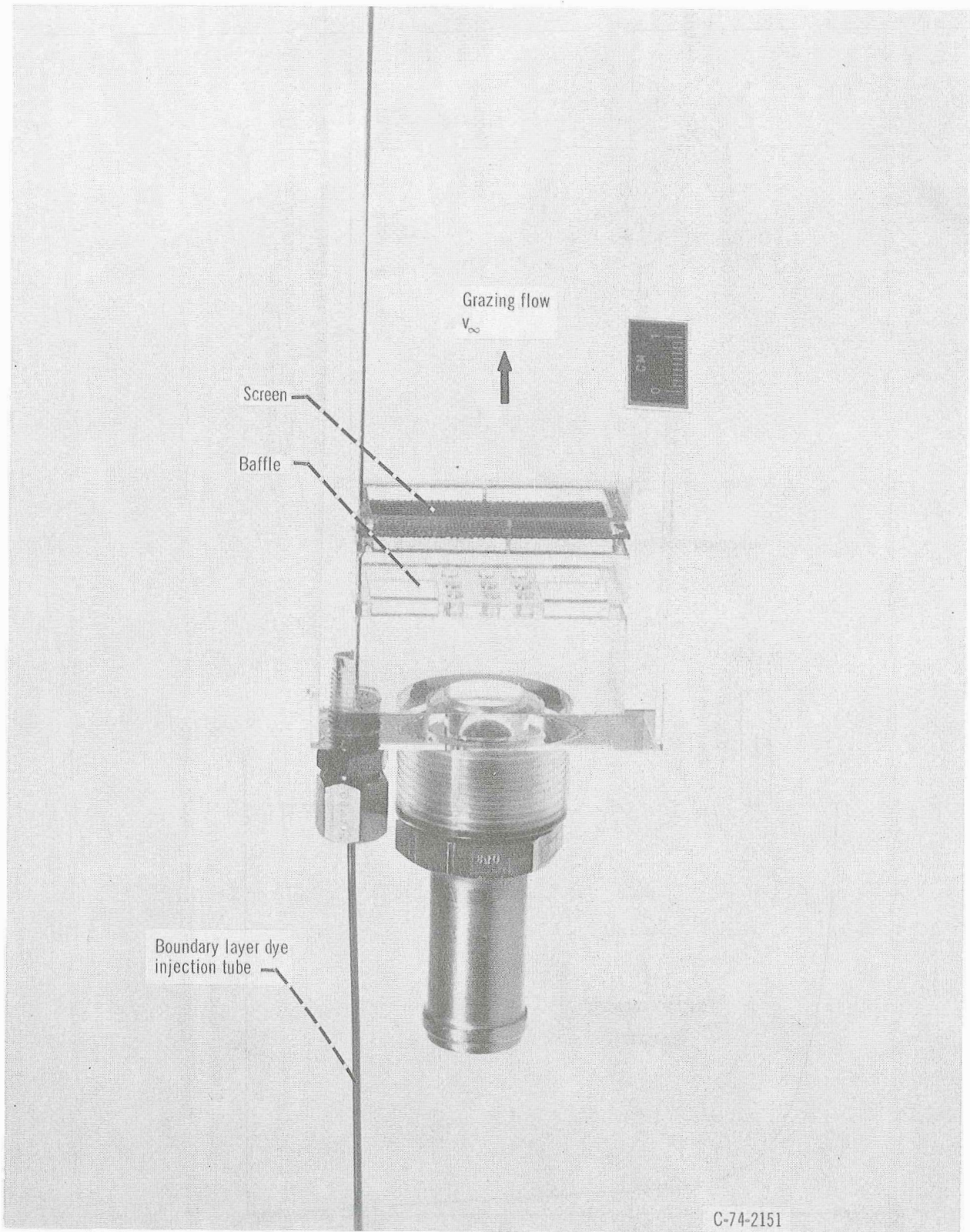


Figure 4. - Flow channel entrance.

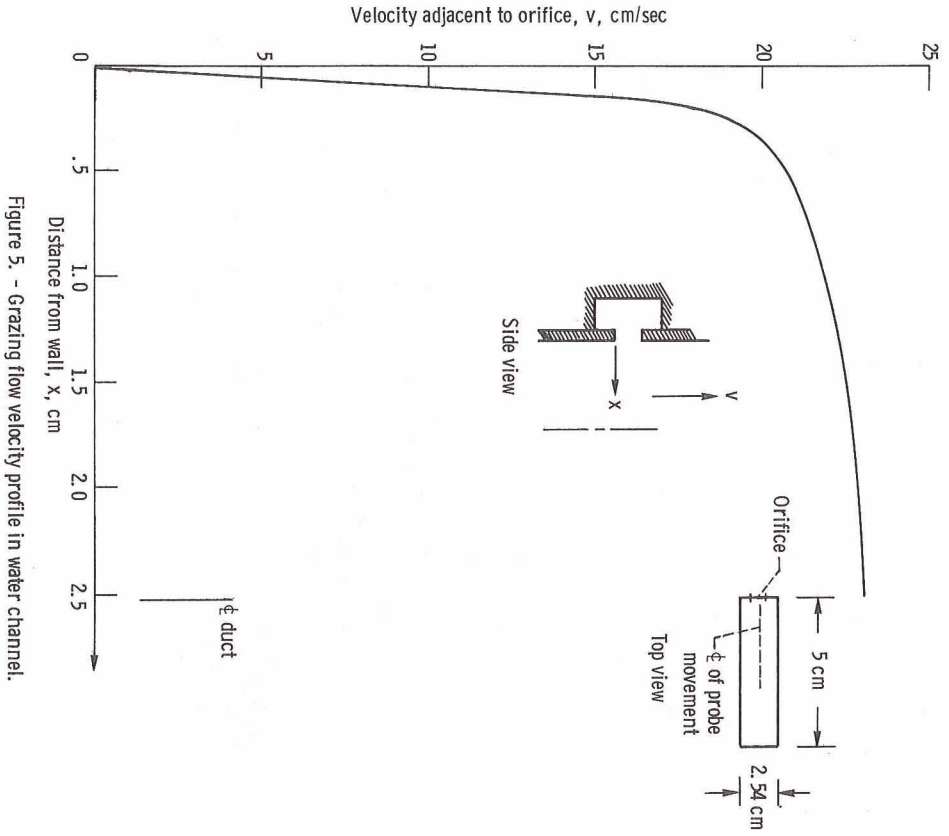


Figure 5. - Grazing flow velocity profile in water channel.

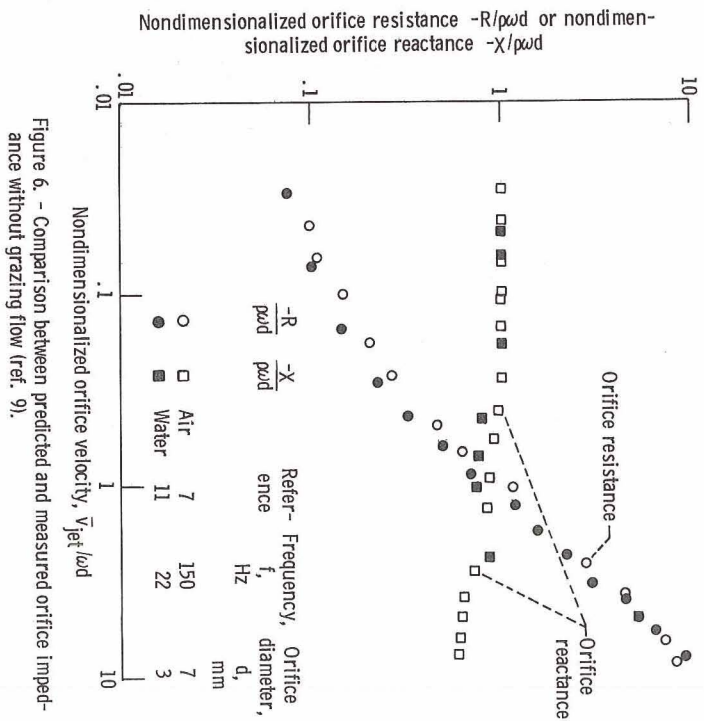


Figure 6. - Comparison between predicted and measured orifice impedance without grazing flow (ref. 9).

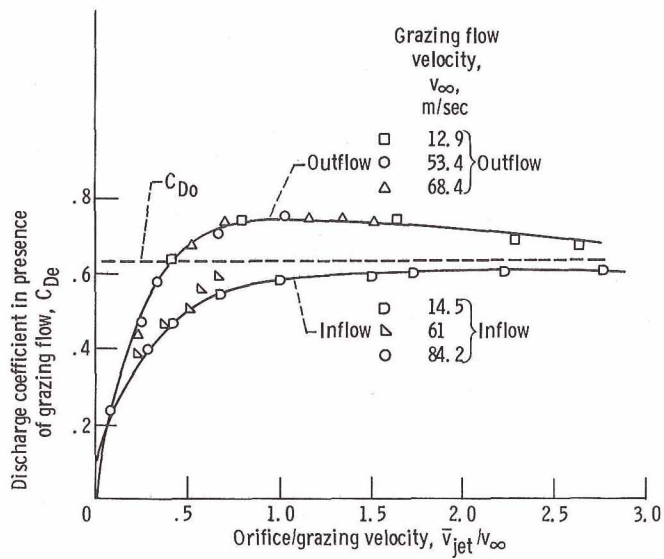
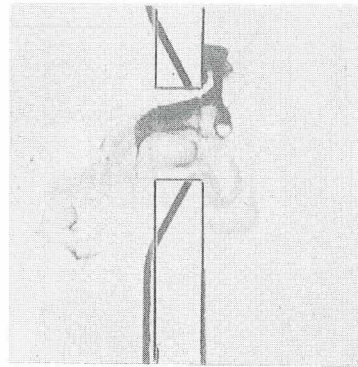


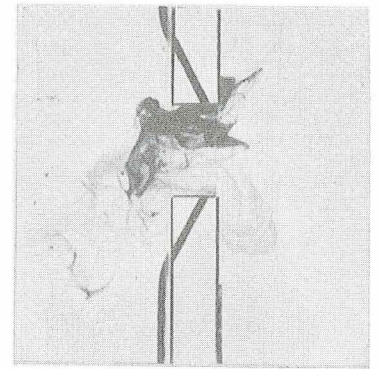
Figure 7. - Typical correlation of orifice discharge coefficient data with grazing flow (from ref. 6).



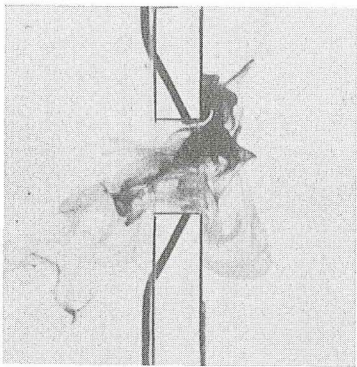
t = 0 sec
Start of outflow



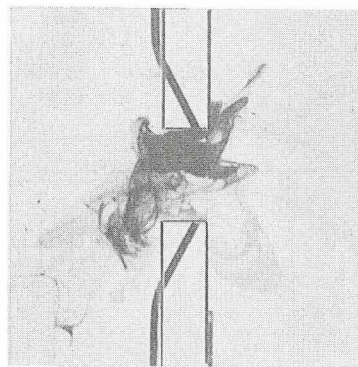
t = 0.2 sec



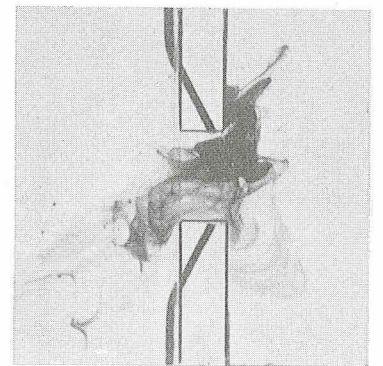
t = 0.54 sec
End of first
complete cycle



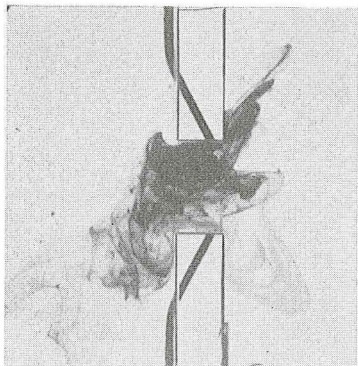
t = 0.77 sec



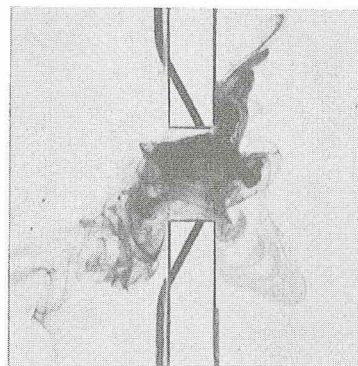
t = 1.05 sec
End of second
cycle



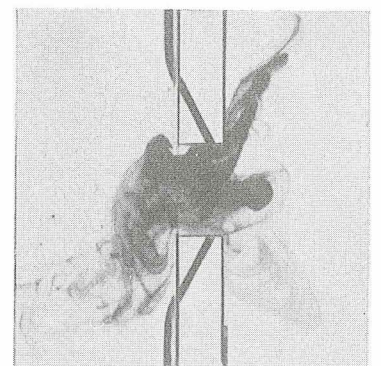
t = 1.25 sec



t = 1.58 sec
End of third
cycle



t = 1.76 sec



t = 2.17 sec
End of fourth
cycle

Figure 8. - Linear (viscous) flow regimes in absence of grazing flow for low amplitude oscillating orifice flow at 2 hertz.

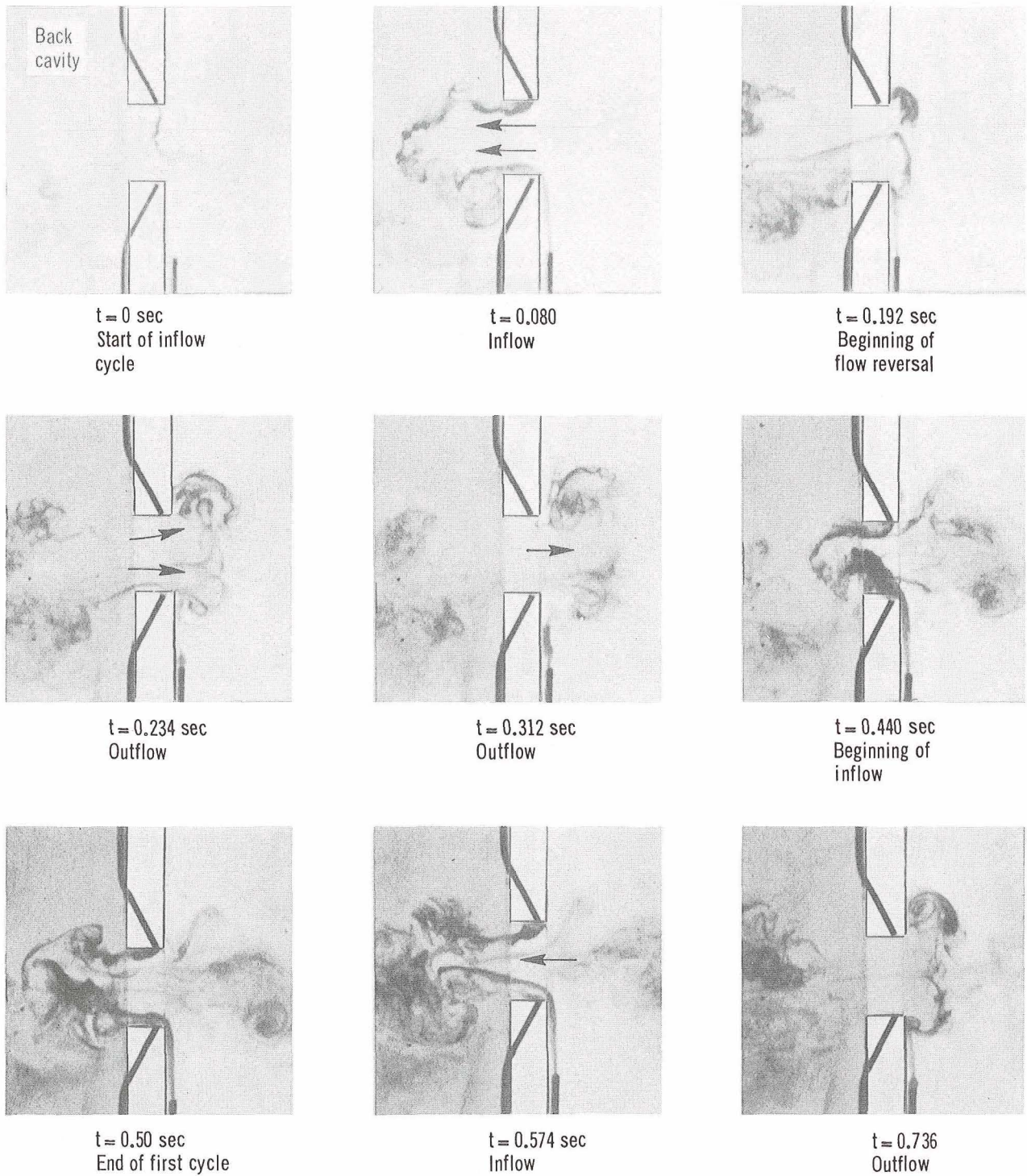
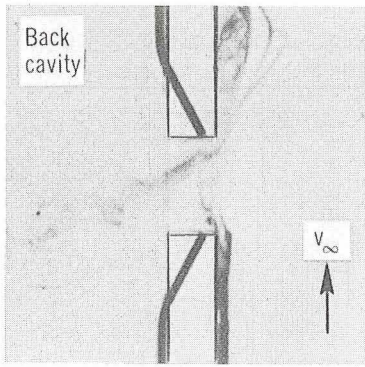
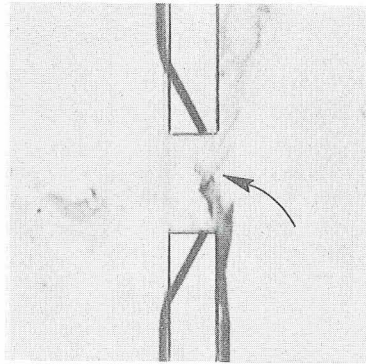


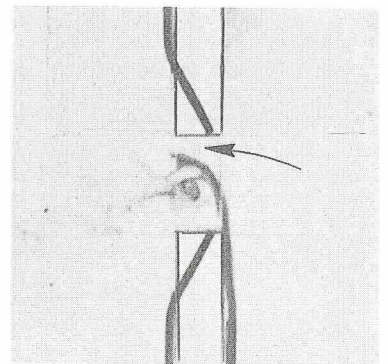
Figure 9. - Nonlinear flow regimes in absence of grazing flow for high amplitude oscillating orifice flow at 2 hertz.



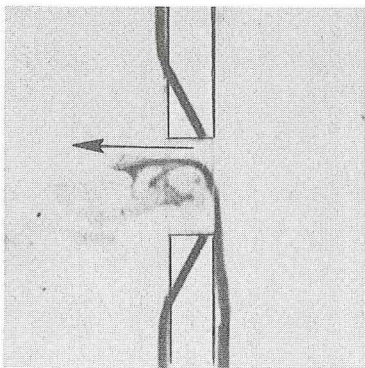
t = 0 sec
Start of
cycle



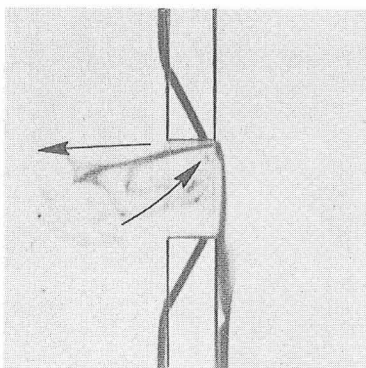
t = 0.061 sec
Beginning of
inflow



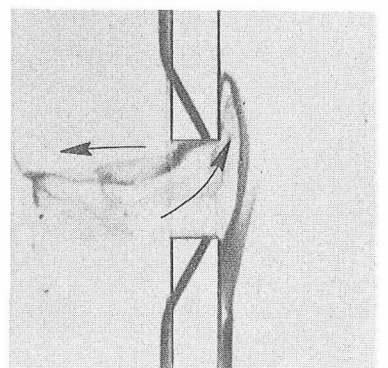
t = 0.122 sec
Inflow



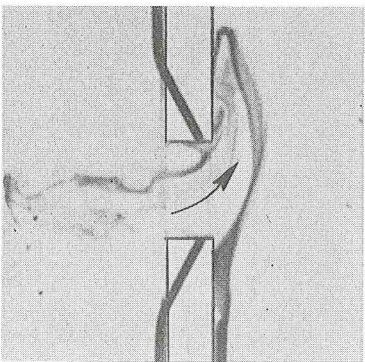
t = 0.178 sec
Inflow



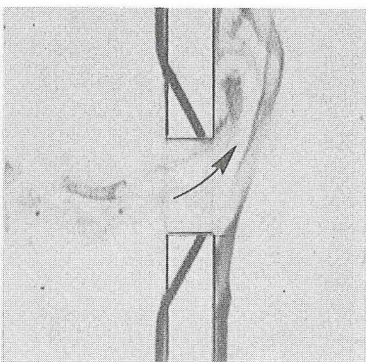
t = 0.236 sec
Beginning of
flow reversal



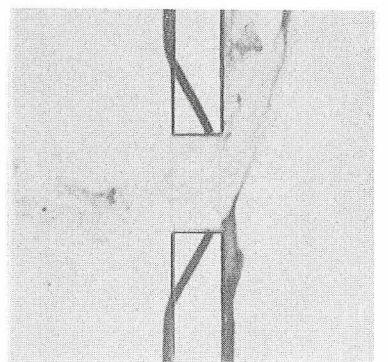
t = 0.312 sec
Outflow



t = 0.364 sec
Outflow



t = 0.44 sec
End of outflow



t = 0.5 sec
Beginning of
new cycle

Figure 10. - Nonlinear flow regimes with 0.3-meter-per-second grazing flow and intermediate amplitude oscillating orifice flow at 2 hertz.

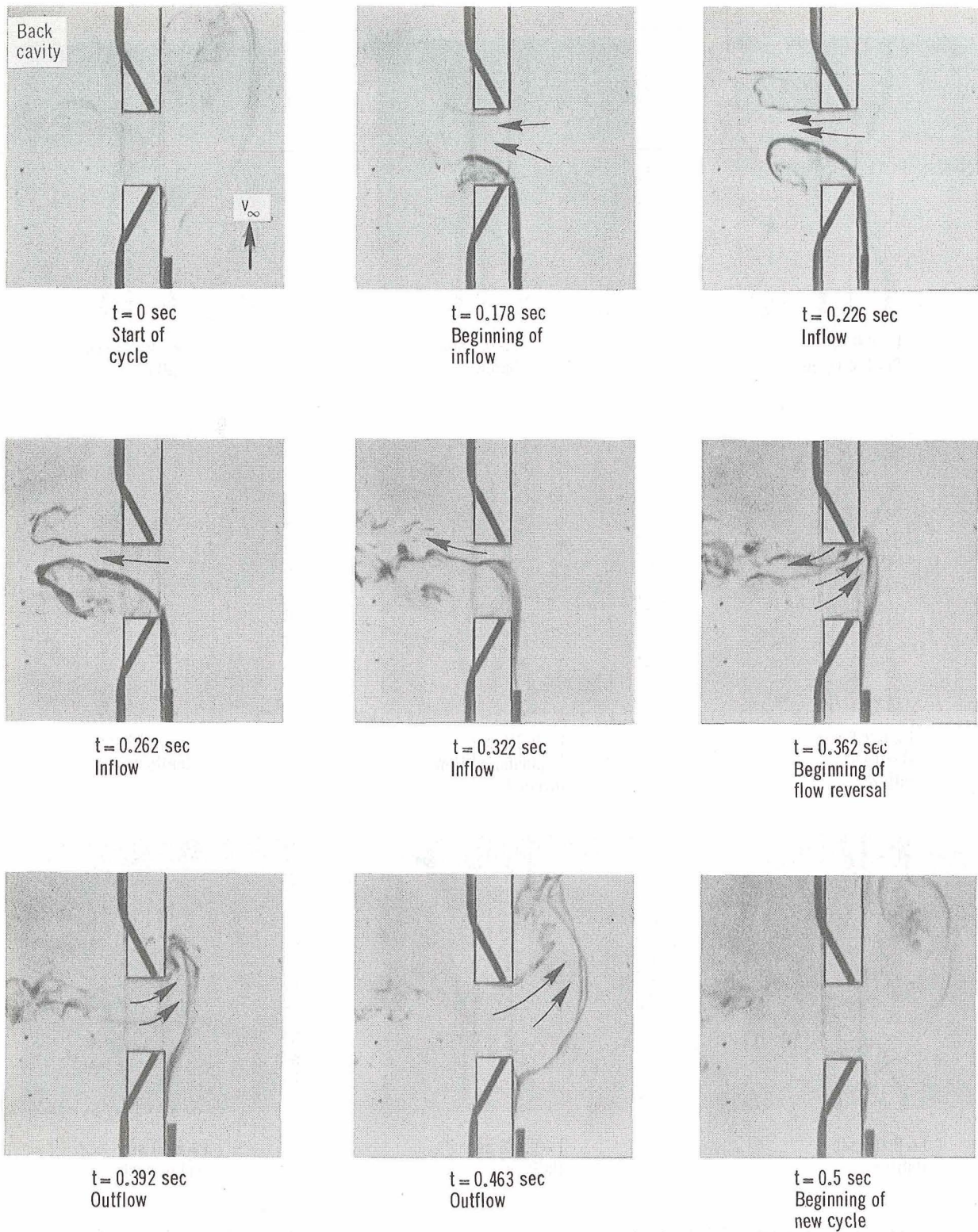
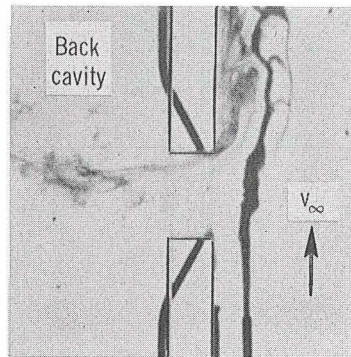
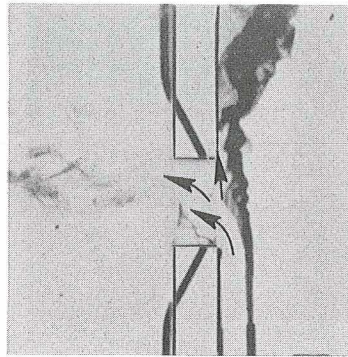


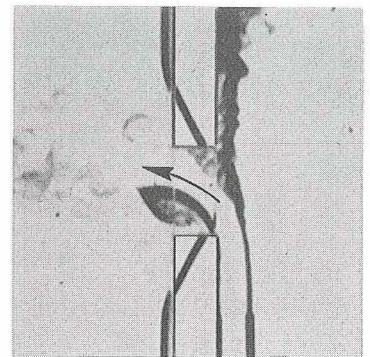
Figure 11. - Nonlinear flow regimes with 0.3-meter-per-second grazing flow and moderately high amplitude oscillating flow at 2 hertz.



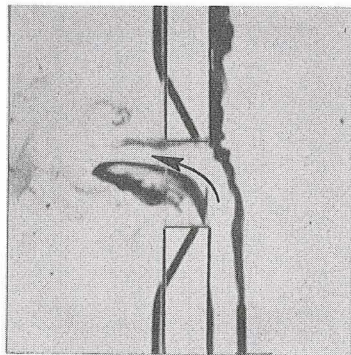
t = 0.0 sec
Start of cycle



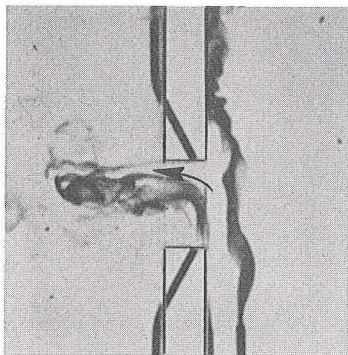
t = 0.1 sec
Inflow



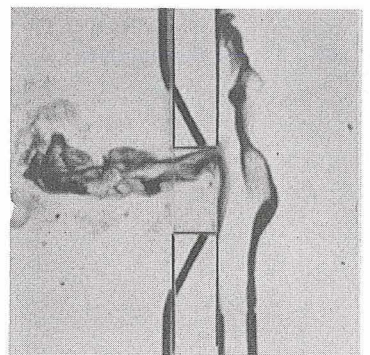
t = 0.218 sec
Inflow



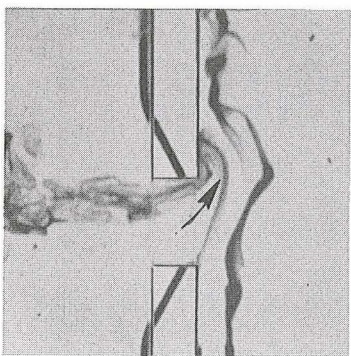
t = 0.268 sec
Maximum inflow



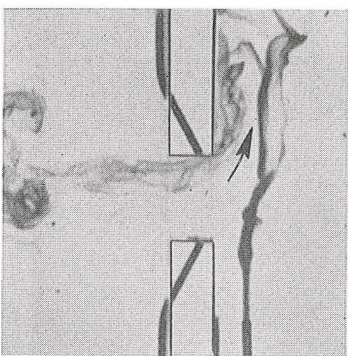
t = 0.316 sec
Beginning of flow reversal



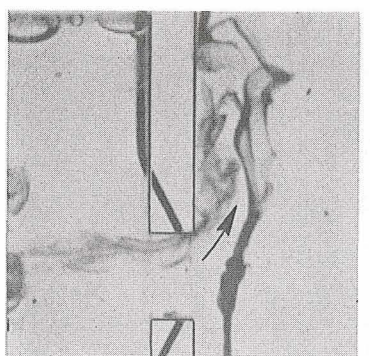
t = 0.364 sec
Outflow



t = 0.404 sec
Outflow

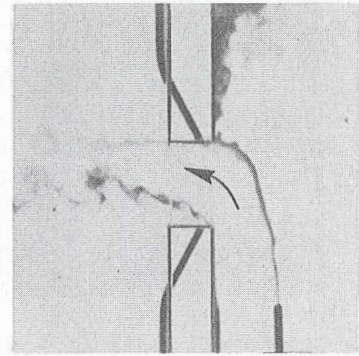
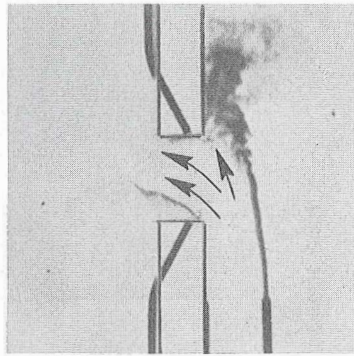
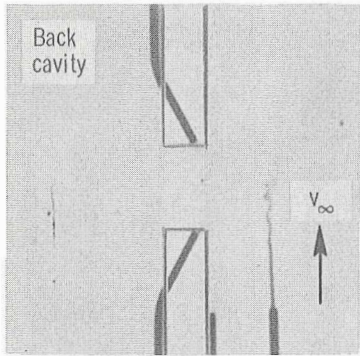


t = 0.476 sec
Outflow



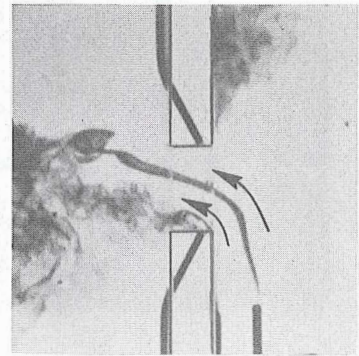
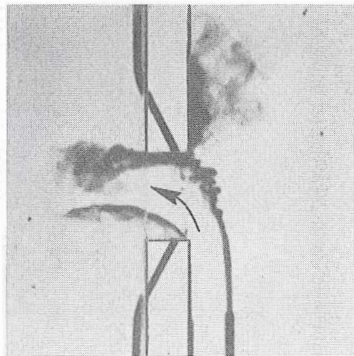
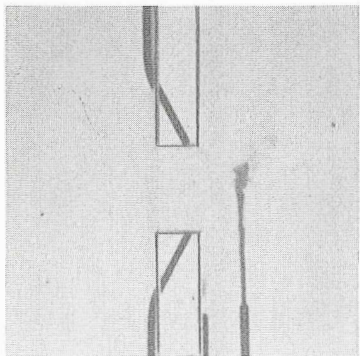
t = 0.50 sec
End of cycle

Figure 12. - Nonlinear flow regimes with 0.3-meter-per-second grazing flow and intermediate amplitude oscillating flow at 2 hertz with dye trace of stream tube at maximum distance from wall for which capture by hole can occur.



Start of cycle → Increasing time

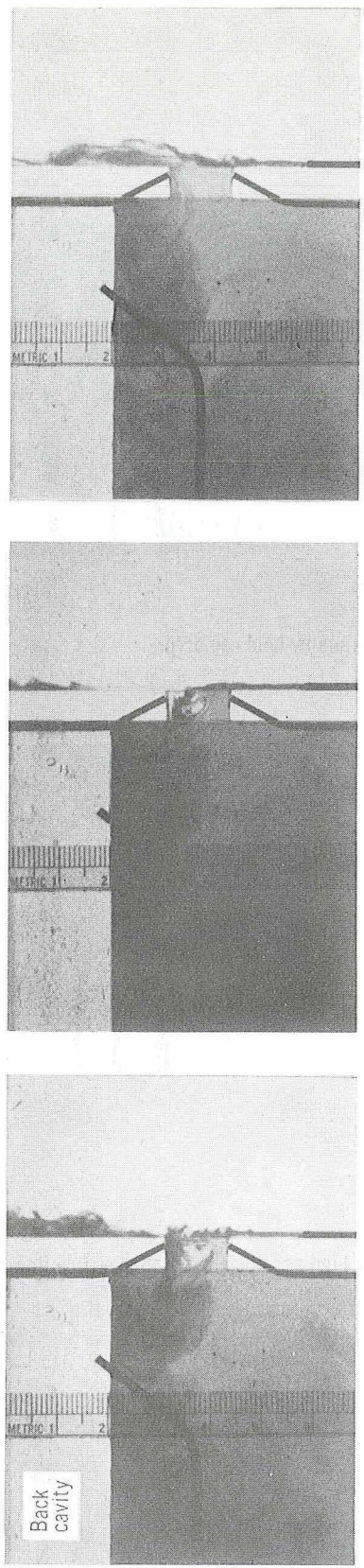
(a) Dye trace of stream tube at maximum distance from wall for which capture by hole can occur.



Start of cycle → Increasing time

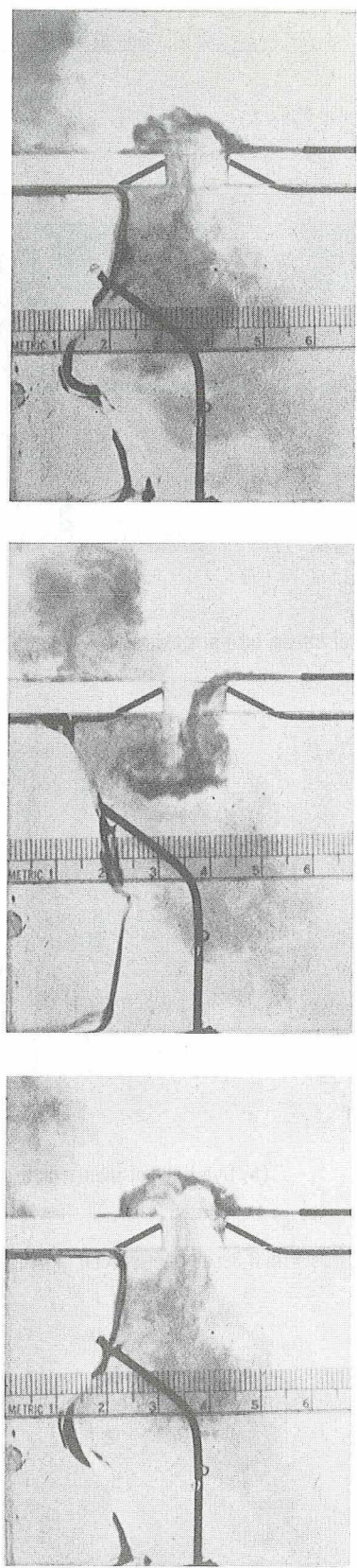
(b) Dye trace of intermediate captured streamline.

Figure 13. - Nonlinear flow regimes with 0.3-meter-per-second grazing flow and moderately high amplitude oscillating orifice flow at 2 hertz.



Start of cycle → Increasing time

(a) 1-Hertz oscillation with 2-centimeter depth of air in back cavity (0.5 amplitude level).



Start of cycle → Increasing time

(b) 5-Hertz oscillation resonance in back cavity with 2-centimeter depth of air in back cavity (0.2 amplitude level).

Figure 14. - Nonlinear flow regimes with 0.3-meter-per-second grazing flow and intermediate amplitude oscillating orifice flow applied to main channel flow.

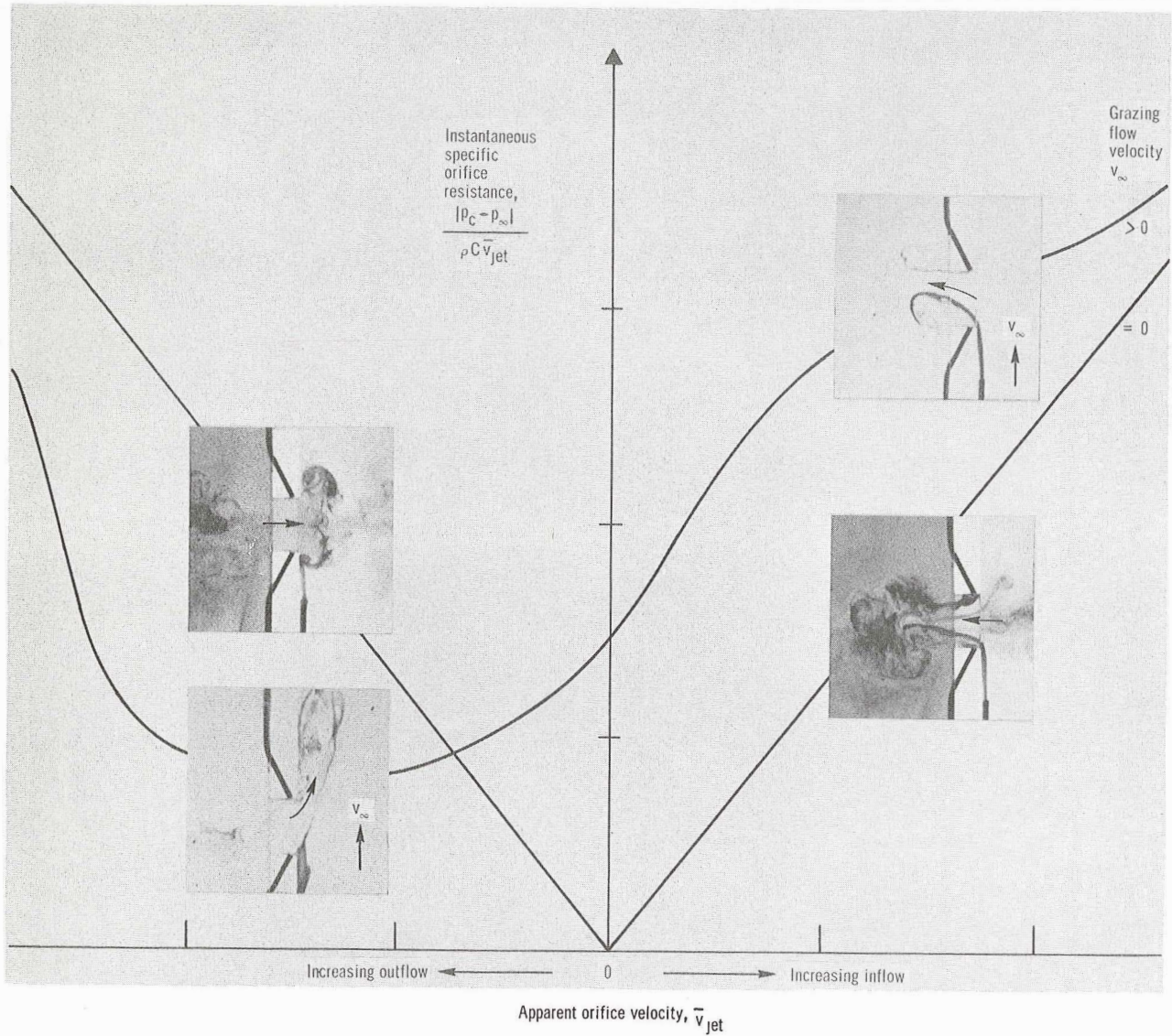


Figure 15. - Schematic of effect of sinusoidally varying orifice flow rate on instantaneous specific orifice resistance and flow profiles.



POSTMASTER: If Undeliverable (Section 158
Postal Manual) Do Not Return

"The aeronautical and space activities of the United States shall be conducted so as to contribute . . . to the expansion of human knowledge of phenomena in the atmosphere and space. The Administration shall provide for the widest practicable and appropriate dissemination of information concerning its activities and the results thereof."

—NATIONAL AERONAUTICS AND SPACE ACT OF 1958

NASA SCIENTIFIC AND TECHNICAL PUBLICATIONS

TECHNICAL REPORTS: Scientific and technical information considered important, complete, and a lasting contribution to existing knowledge.

TECHNICAL NOTES: Information less broad in scope but nevertheless of importance as a contribution to existing knowledge.

TECHNICAL MEMORANDUMS: Information receiving limited distribution because of preliminary data, security classification, or other reasons. Also includes conference proceedings with either limited or unlimited distribution.

CONTRACTOR REPORTS: Scientific and technical information generated under a NASA contract or grant and considered an important contribution to existing knowledge.

TECHNICAL TRANSLATIONS: Information published in a foreign language considered to merit NASA distribution in English.

SPECIAL PUBLICATIONS: Information derived from or of value to NASA activities. Publications include final reports of major projects, monographs, data compilations, handbooks, sourcebooks, and special bibliographies.

TECHNOLOGY UTILIZATION PUBLICATIONS: Information on technology used by NASA that may be of particular interest in commercial and other non-aerospace applications. Publications include Tech Briefs, Technology Utilization Reports and Technology Surveys.

Details on the availability of these publications may be obtained from:

SCIENTIFIC AND TECHNICAL INFORMATION OFFICE

NATIONAL AERONAUTICS AND SPACE ADMINISTRATION

Washington, D.C. 20546